Available online at www.sciencedirect.com
SCIENCE DIRECT®
Physica B 371 (2006) 241–244
PHYSICA B
www.elsevier.com/locate/physb

Small polarons as charge carriers in the transport of $(La_{1/3}Sm_{2/3})_{0.67}Ba_{0.33-x}Sr_xMnO_3$ ($x = 0$, 0.1, 0.2 and 0.33)

Saket Asthana[a], D. Bahadur[a,*], C.M. Srivastava[b]

[a]*Department of Metallurgical Engineering and Materials Science, Indian Institute of Technology, Mumbai 400076, India*
[b]*Department of Physics, Indian Institute of Technology, Mumbai 400076, India*

Received 28 August 2005; received in revised form 5 October 2005; accepted 7 October 2005

Abstract

It is shown that charge transport in substituted manganites $(La_{1/3}Sm_{2/3})_{0.67}Ba_{0.33-x}Sr_xMnO_3$ ($x = 0.0$, 0.1, 0.2 and 0.33) is through polarons which are formed through electron–phonon interaction whose strength determines the mobility of the charge carrier. For weak coupling, the free phonon mode is only slightly affected but in strong coupling, the free phonon mode disappears and 'displaced' phonon modes appear. This is seen directly in IR spectra.

PACS: 75.47.Lx; 72.90.+y

Keywords: Manganites; Small polaron; Transport mechanism; IR spectra; Displaced phonons

1. Introduction

The nature of the charge carriers and the mechanism of transport in $(R_{1-x}M_x)MnO_3$ manganites (R = Nd, Pr, Sm, La and M = Ba, Sr, Ca) has been extensively investigated [1–6] but there is still no theory that can satisfactory account for the complex correlation between the magnetic and transport properties of the system. Since most attempts to understand the physics of the problem relate to the competition between the double exchange and super-exchange [7–11], the fraction x depending on the concentration of the divalent alkaline earth metal atom and it becomes important as it governs the dominance of one interaction over the other. For example, the half-doped manganites ($x = 0.5$) which are at the threshold of ferromagnetic to antiferromagnetic phase transition at low temperature comprise of regions with three different microscopic magnetic phases and two crystallographic structures simultaneously coexisting [12]. To explore the nature of the charge carriers, we have therefore chosen $x = 0.33$. In this case, there is a single magnetic phase transition at T_c as it is cooled from 300 K to low temperature and there is no first-order phase transition of crystallographic phase. However, there is a strong dependence of the mobility of the charge carriers on temperature depending on the average ionic radius of the A-site ion, $\langle r_A \rangle$. The $\langle r_A \rangle$ is directly related to the tolerance factor which is defined as $\tau = \langle r_A \rangle + r_O/\sqrt{2}(r_B + r_O)$. Here, r_O and r_B are the ionic radii of the oxygen ion and B-site ion, respectively. Amongst others, this is also reported by Garcia-Munoz et al. [13] who have observed in $(R_{1-x}R'_x)_{2/3}A_{1/3}MnO_3$ (A = Ca, Sr) variation of residual resistivity, $\rho(0)$ by six orders (10^{-3}–$10^3\,\Omega$ cm) when average A-site ion radius, $\langle r_A \rangle$, decreases from 1.20 to 1.11 Å.

Ramakrishnan [14] has attempted to account for it by empirically adding a factor $\exp[\lambda\delta M/M_s]$ to Mott's minimum resistivity, $\hbar a/e^2$, where a is the lattice constant and the expression is based on the uncertainty relationship for hopping charge carriers, giving $\rho_{min} \sim 10^{-3}\,\Omega$ cm observed in manganites. Here, δM is the deviation from the saturation magnetization, M_s, and λ is a large constant. Though the exponential term is based on experimental observation, the magnetic origin for localization is difficult to understand. We show that a similar result is obtained in $(La_{1/3}Sm_{2/3})_{0.67}Ba_{0.33-x}Sr_xMnO_3$ as x is varied from 0 to

*Corresponding author. Tel.: +91 22 25767632; fax: +91 22 25723480.
E-mail address: dhirenb@iitb.ac.in (D. Bahadur).

0921-4526/$ - see front matter © 2005 Elsevier B.V. All rights reserved.
doi:10.1016/j.physb.2005.10.113

0.33. This composition is chosen to study the dependence of the mobility of the charge carrier on only one parameter, the average size of the A-site ion, $\langle r_A \rangle$, as Ba and Sr are from the same group but their ionic radii are substantially different, 1.61 Å and 1.44 Å, respectively. The residual resistivity varies from 0.6 to $10^6\,\Omega$ cm with $\langle r_A \rangle$ increasing from 1.15 to 1.20 Å. We show below that the variation in the residual resistivity, $\rho(0)$, with $\langle r_A \rangle$ is mainly due to the polaron–polaron interaction energy [15]. In this model, the active free phonon that is coupled to the electron forming the small polaron has its frequency shifted to that of displaced phonons. In the weak electron–phonon coupling, the change in free phonon spectrum is small but in the case of strong coupling, it is clearly noticeable in IR spectra. We further show that the frequency of the active phonon mode obtained from the resistivity data agrees with those obtained from IR measurement for the displaced phonons.

2. Theory

Zener obtained a relation between electrical conductivity and double exchange which is similar to Einstein expression for a diffusion species with a temperature-independent diffusion constant,

$$\sigma = \frac{ne^2}{ah}\frac{T_c}{T} = ne\mu, \tag{1}$$

$$\mu = \frac{eD}{k_B T}, \quad D = D_0 = \frac{ek_B T_c}{ah}, \tag{2}$$

where n is the number of Mn^{4+} ions and D is the diffusion coefficient [16]. One of the authors has treated the charge transport in manganite in detail [17]. We show here in this model that the transport in the high-temperature limit is dominated by thermally activated hopping and in the low-temperature limit by tunneling assisted by the zero-point vibrations and hence an electronic phase transition occurs at the switch over temperature.

We treat the charge carriers as small polarons and describe them by the Holstein Hamiltonian used in Ref. [18]:

$$H = \sum_i \varepsilon_i c_i^+ c_i + \sum_{ij} t_{ij}(c_{i+j,\sigma}\, c_{i,\sigma} + HC) + \sum_q \omega_q a_q^+ a_q + \sum_{qi} g_{iq} c_i^+ c_i (a_q^+ + a_q). \tag{3}$$

Here, t_{ij} is the electron transfer integral, g_{iq} the electron–phonon coupling constant, ε_i the electron energy at site i, ω_q the energy of free phonon, and $c_i(c_i^+)$ and $a_i(a_i^+)$ are electron and phonon annihilation (creation) operators, respectively. The polaron canonical transformation yields [15,18]

$$H_{\text{eff}} = \sum_i (\varepsilon_i - \varepsilon_p) l_i^+ l_i + \sum_{i,j} (t_{ij} l_i^+ l_j X_{ij} + HC) + \sum_q \omega_q b_q^+ b_q, \tag{4}$$

$$\varepsilon_p = \sum_q \langle g_{iq}^2 \rangle / \omega_q, \tag{5}$$

where l_i^+ creates a polaron at site i, X_{ij} are the Franck–Condon transition between sites i and j, ε_p is the polaron stabilization energy and b_q^+ is a creation operator for displaced phonons, the displacement determined by the position of all electrons,

$$b_q^+ = a_q^+ + \sum_i g_{iq} e^{iq.R_i} c_i^+ c_i. \tag{6}$$

The detailed analysis of Franck–Condon transitions shows that polarons at one site interact with that at the neighbouring site and hopping can occur only if one site is occupied and the other is vacant. This gives a factor $\text{sech}^2(\varepsilon_p/2T)$ in the mobility of the polaron. The other temperature-dependent factor that enters the mobility is the activation energy $U_0 = (1/4)n_{ph}\omega_{ph}$ where n_{ph} is the average number of phonons in the polaron cloud. For the electron to jump from site R_i to R_j, this adds a factor $\exp(-U_0\langle \sin^2 1/2\, \underline{\boldsymbol{q}} \cdot \underline{\boldsymbol{a}} \rangle) = \exp(-U_0\xi^2/T)$ where $\underline{q}$ is the wave vector and $\underline{\boldsymbol{a}} = \underline{\boldsymbol{R}}_i - \underline{\boldsymbol{R}}_j$ is the displacement vector for the jump [16,17]. Following Kubo's current–current correlation formulation, Reik [18] has obtained H_{eff} to obtain an expression for DC resistivity which has been adopted for transport in manganites using the correlated polaron approximation [17],

$$t_{ij} = t, \quad 1/t = \bar{\theta}_D = \omega_{ph}\left\langle \sin^2 \frac{1}{2}\underline{\boldsymbol{q}} \cdot \underline{\boldsymbol{a}} \right\rangle = \omega_{ph}\xi^2, \tag{7}$$

$$\rho_c^{hop} = \frac{AT}{n}[1 + c(1 - m^2(t))\sigma_a^2]\cosh^2(\varepsilon_p/2T) \times \exp[U_0(1 - m^k)\sigma_a^2/T], \quad T > \bar{\theta}_D/4, \tag{8}$$

with $m(t) = M(T)/M(0)$, n is the number density of charge carriers, and c and k are constants depending on the strength of the spin–spin scattering in polaron transport. Here, $A = 2k_B/\sqrt{\pi}\omega_{ph}a^2e^2$, ω_{ph} is the frequency of the active phonon, a the lattice constant, and σ_a is the short-range atomic order parameter that varies with T as $(1 - 0.75t_{ca}^3)^{1/2}$ where $t_{ca} = T/T_{ca}$. Eq. (8) is similar to that obtained for glassy semiconductor ($m(t) = 0$) by Mott [19] for $T > \bar{\theta}_D/4$. For $T < \bar{\theta}_D/4$, quantum effects dominate over classical effects and according to Mott, due to processes like variable range hopping and Anderson localization, as T tends to zero, charge transport is through tunneling and ρ increases as $A' \exp(b/T^{1/4})$. This is clearly not applicable to manganites where for the same number of charge carriers (x = constant) and nearly identical room-temperature resistivity, the residual resistivity, $\rho(0)$, changes from 10^{-3} to $10^3\,\Omega$ cm if $\langle r_A \rangle$ is varied [13,14]. We show that the residual resistivity is proportional to $\cosh^2(2\varepsilon_p/\bar{\theta}_D)$ where ε_p is the polaron binding energy in Eq. (8) and $\bar{\theta}_D$ is the Debye temperature relating to the displaced phonon given by Eq. (7).

The scattering by phonons is proportional to lattice strain, $\langle \delta R^2 \rangle / R^2$, which is equal to $1.6k_BT/Ms^2$ in the high-temperature limit where phonons dominate and to $0.4k_B\theta_D/Ms^2$ in the low-temperature limit where zero point

vibrations dominate. Here, M is the mass of the ion and s is the velocity of sound [20]. We assume, following Mott, that Eq. (8) gives the resistivity for $T<\bar{\theta}_D/4$, by replacing T by $\bar{\theta}_D/4$ in the prefactor and in the cosh term, because the statistical weight of each lattice vibrational mode in electron–phonon scattering due to zero point vibration is the same. We then obtain

$$\rho_c^{hop} = \frac{A\bar{\theta}_D}{4n}[1 + c(1 - m^2(t))\sigma_a^2]\cosh^2(2\varepsilon_p/\bar{\theta}_D) \times \exp[U_0(1 - m^k)\sigma_a^2/T], \quad T<\bar{\theta}_D/4. \tag{9}$$

For $T\to 0$ using $c = 1$ and spin-wave theory,

$$\rho_c^{hop} = \rho(0)[1 + 2\zeta T^{3/2}\sigma_a^2], \tag{10}$$

where ζ is the spin-wave constant and

$$\rho(0) = \frac{A\bar{\theta}_D}{4n}\cosh^2\left(\frac{2\varepsilon_p}{\bar{\theta}_D}\right). \tag{11}$$

With the same parameters A/n, T_c, T_{ca}, $\bar{\theta}_D$, U_0 and $k = 2.3$, $\rho(T)$ is plotted using the high-temperature (Eq. (8)) and the low-temperature (Eq. (9)) limits. This is shown in Fig. 1 for the parameters given in Table 1. First, ε_p is estimated from the high-T plot, $\bar{\theta}_D$ is then estimated using Eq. (11). The variation of $\rho(0)$ with τ for $(R_{1-x}R_x')_{2/3}A_{1/3}MnO_3$ (A = Ca, Sr) is shown in Fig. 2 where the data is from Ref. [13] in which the cosh term tends to 1 for $\varepsilon_p \ll \theta_D/2$ and to ∞ for $\varepsilon_p \gg \theta_D/2$. If $4\varepsilon_p/\bar{\theta}_D\alpha$ ln $\rho(0)\alpha(T - T_c) = \Delta$, where T_c is the value for the structure closest to cubic pervoskite, then from Eq. (11), ln $\rho(0)$ is linearly proportional to Δ. The average τ_c in the present case is nearly 0.895, so $\rho(0)$ increases linearly on both sides of this critical value. As Δ increases, at $T\to 0$, the polarons change from itinerant to localized states since Mn–O–Mn angles deviate more from 180°. From Fig. 2, Δ varies linearly with $4\varepsilon_p/\bar{\theta}_D$. Fig. 3 gives the vibrational spectra of the samples. It is shown that a magnetic and charge-order Bravais lattice exists for $A_{1-x}^{3+}B_x^{2+}Mn_{1-x}^{3+}Mn_x^{4+}O_3$ for $x = n/8$ where n is an integer and the cell constant is $2a$, double that of the chemical cell [17]. Correlated polarons transport in manganites with $x = 1/3$ occurs with the lattice vibrational mode with frequency $\omega_{ph} = 5.5\times10^{12}$ Hz [17]. This nearly corresponds to the 179 cm^{-1} bond stretching mode in which the two oxygen atoms move along the bond direction $\pm z$ in the MnO_6 octahedra with all other four oxygen atoms surrounding the Mn atom remaining silent

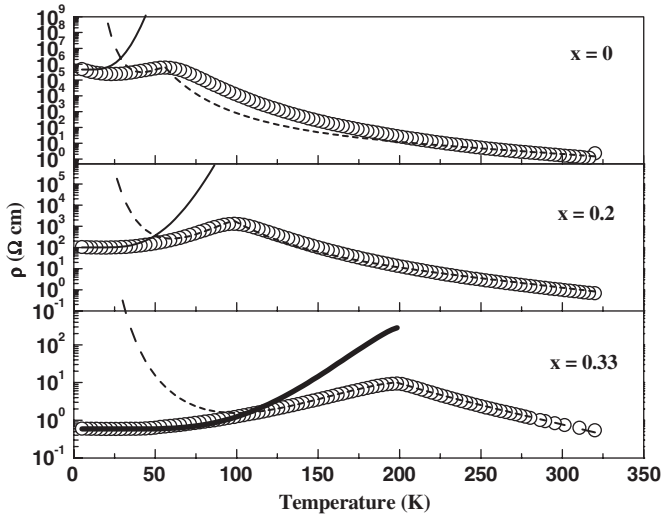

Fig. 1. Observed $\rho(T)$ curves for $(La_{1/3}Sm_{2/3})_{0.67}Ba_{0.33-x}Sr_xMnO_3$ ($x = 0$, 0.2 and 0.33) are shown in hollow circles. The fitted plots are shown by dotted lines (- - -) for the high-temperature (Eq. (8)) and by solid lines (—) for the low-temperature (Eq. (9)) limit.

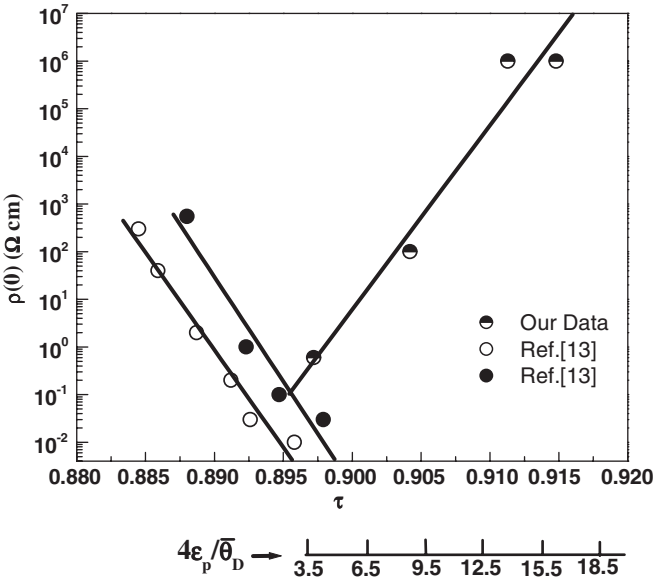

Fig. 2. Variation of $\rho(0)$ with tolerance factor (τ) for $(La_{1/3}Sm_{2/3})_{0.67}Ba_{0.33-x}Sr_xMnO_3$ ($x = 0$, 0.1,0.2 and 0.33) and data for $(R_{1-x}R'_x)_{2/3}A_{1/3}MnO_3$ (A = Ca (hollow circles), Sr (half-filled circles)) taken from Ref. [13]. The values of $4\varepsilon_p/\bar{\theta}_D$ for our data using Eq. (11) and Table 1 are also given.

Table 1
The fitted parameters, ε_p, $\bar{\theta}_D$, U_0 and n are given for the series $(La_{1/3}Sm_{2/3})_{0.67}Ba_{0.33-x}Sr_xMnO_3$ ($x = 0$, 0.1,0.2 and 0.33)

x	T_{ca} (°K)	A/n (10^{-3}/cm^3)	ε_p (°K)	$\bar{\theta}_D$ (°K)	U_0 (°K)	k	n ($\times10^{18}$/cm^3)
0	310	1.8	500	115	420	2.3	4.1
0.1	310	1.8	470	125	500	2.3	4.1
0.2	310	1.0	450	200	600	2.3	7.4
0.33	310	0.6	380	430	750	2.3	12.4

The value of A/n has been obtained from the $\rho(0)$ values using ω_{ph}^1 with $a = 3.858$ Å.

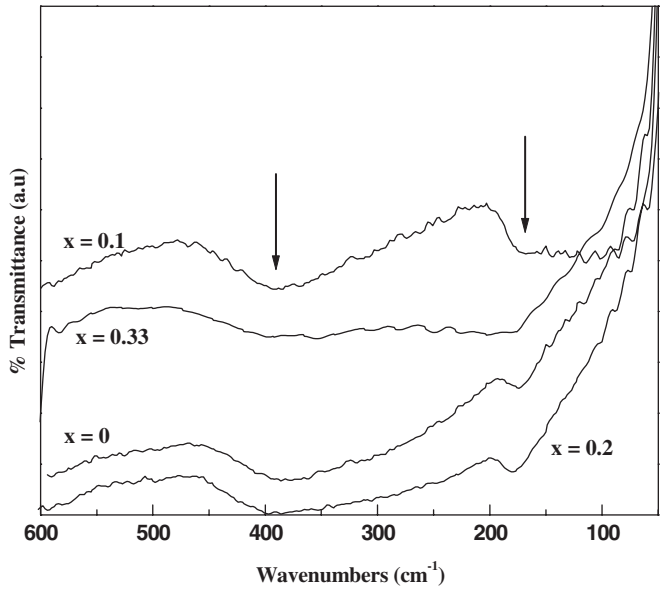

Fig. 3. IR spectra of $(La_{1/3}Sm_{2/3})_{0.67}Ba_{0.33-x}Sr_xMnO_3$ ($x = 0$, 0.1, 0.2 and 0.33). The arrows denote the stretching ($\omega^1_{ph}\sim179\,cm^{-1}$) and bending ($\omega^2_{ph}\sim395\,cm^{-1}$) phonon peaks.

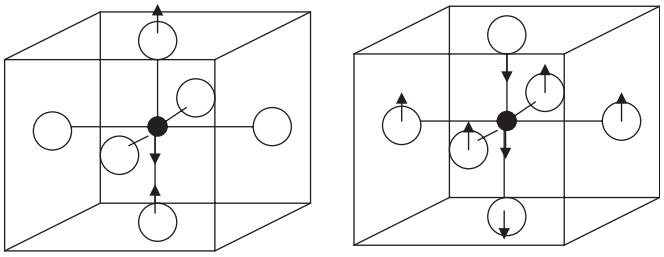

(a) ω^1_{ph} (179 cm^{-1}) (b) ω^2_{ph} (395 cm^{-1})

Fig. 4. The MnO stretching ($\omega^1_{ph}\sim179\,cm^{-1}$) and bending plus stretching ($\omega^2_{ph}\sim395\,cm^{-1}$) vibration modes similar to those observed in $SrTiO_3$ [20] are shown for the present system.

(Fig. 4a). From Table 1, $\bar{\theta}_D/\omega^1_{ph} = 0.42$, 0.47 and 0.74 for $x = 0$, 0.1 and 0.2, respectively, so from Eq. (7), $\langle \sin^2 1/2\,\underline{\boldsymbol{q}}\cdot\underline{\boldsymbol{a}}\rangle$ lies between 0.4 and 0.74. On the other hand, for $x = 0.33$ which has largest mobility as $T\to0$, $\bar{\theta}_D/(\omega^1_{ph}+\omega^2_{ph})$ has a value equal to 0.72. In this case, both the modes of vibration, the MnO stretching ($\omega^1_{ph}\sim179\,cm^{-1}$) and bending plus stretching ($\omega^2_{ph}\sim395\,cm^{-1}$) are similar to that observed for $SrTiO_3$ [21] and appear to be active (Fig. 4). In the Bravais lattice of cell constant $2a$, ω^1_{ph} and ω^2_{ph} modes could exist amongst edge-sharing octants and $\bar{\theta}_D = 0.72(\omega^1_{ph}+\omega^2_{ph})$.

Fig. 3 shows the disappearance of the phonon modes ω^1_{ph} and ω^2_{ph} in the present system for $x = 0.33$ due to strong electron–phonon coupling g_{iq} in Eq. (6) which leads to the appearance of displaced phonons with considerably reduced intensity that play a dominant role in the charge transport process. From Eq. (11), the mobility as $T\to0$ is proportional to $\mathrm{sech}^2(2\varepsilon_p/\bar{\theta}_D)$ and hence is exponentially dependent on $4\varepsilon_p/\bar{\theta}_D$ for $\varepsilon_p/\bar{\theta}_D \geqslant 1$. As ε_p is nearly independent of x, it is $\bar{\theta}_D$ that controls the low-temperature transport; lower the $\bar{\theta}_D$, the lower the mobility and hence higher the residual resistivity.

References

[1] B. Raveau, S. Hebert, A. Maignan, R. Fresard, M. Hervieu, D. Khomskii, J. Appl. Phys. 90 (2001) 1297.
[2] Y. Tokura, H. Kuwahara, Y. Moritomo, Y. Tomioka, A. Asamitsu, Phys. Rev. Lett. 76 (1996) 3184.
[3] S. Asthana, D. Bahadur, A.K. Nigam, S.K. Malik, J. Phys.: Condens. Matter 16 (2004) 5297.
[4] A. Asamitsu, Y. Moritomo, R. Kumai, Y. Tomioka, Y. Tokura, Phys. Rev. B 54 (1996) 1716.
[5] L.M. Rodriguez-Martinez, J.P. Attfield, Phys. Rev. B 54 (1996) 15622.
[6] C.M. Srivastava, R.K. Dwivedi, S. Asthana, A.K. Nigam, D. Bahadur, J. Magn. Magn. Mater. 284 (2004) 239.
[7] H. Kuwahara, Y. Tomioka, A. Asamitsu, Y. Moritomo, Y. Tokura, Science 270 (1995) 961.
[8] P.G. de Gennes, Phys. Rev. 118 (1960) 141.
[9] C. Zener, Phys. Rev. 82 (1951) 403.
[10] P.W. Woodword, D.E. Cox, T. Vogt, C.N.R. Rao, A.K. Cheetan, Chem. Mater. 11 (1999) 358.
[11] C. Ritter, R. Mahendiran, M.R. Ibarra, L. Morellon, A. Maignan, B. Raveau, C.N.R. Rao, Phys. Rev. B 61 (2000) R9229.
[12] R. Kajimoto, H. Yoshizawa, H. Kawano, H. Kuwahara, Y. Tokura, Phys. Rev. B 60 (1999) 9506.
[13] J.L. Garcia-Munoz, J. Fontcuberta, B. Martinez, A. Seffar, S. Pinol, X. Obradors, Phys. Rev. B 55 (1997) R668.
[14] T.V. Ramakrishnan, in: C.N.R. Rao, B. Raveau (Eds.), Colossal Magnetoresistance, Charge Ordering and Related properties of Mangnese Oxides, World Scientific, Singapore, 1998, pp. 325–345.
[15] C.M. Srivastava, Pramana J. Phys. 50 (1998) 11.
[16] C. Zener, Phys. Rev. 82 (1951) 403.
[17] C.M. Srivastava, J. Phys.: Condens. Matter 11 (1999) 4539.
[18] H.G. Reik, in: J.T. Devreese (Ed.), Polarons in Ionic Crystals and Polar Semiconductors, Amsterdam, North-Holland, 1972, pp. 679–714.
[19] N.F. Mott, E.A. Davis, Electronic Processes in Non-crystalline Materials, second ed., Clarendon, Oxford, 1979.
[20] D. Pines, Elementary Excitations in Solids, W.A. Benjamin, Inc., New York, 1964.
[21] J.R. Durig (Ed.), Vibrational Spectra and Structure, vol. 9, Marcel Dekker, New York, 1972, p. 90.